

A NOVEL INTERACTIVE CO-SEGMENTATION APPROACH FOR EXTRACTION OF FEATURES OF AN IMAGE

Kulli Joshibabu B.Tech, (M.Tech)¹

¹Department Of CSE, Acharya Nagarjuna University

Guntur, AP

Email ID: joshi.k525@gmail.com

Ummadi Sathish Kumar M.Tech (Ph.d)²

²Assistant Professor, Acharya Nagarjuna university

Guntur, AP

Email ID: sathishummadi@gmail.com

Abstract A new interactive image co segmentation algorithm using possibility estimation and higher order energy is proposed for extracting general foreground objects from a group of interrelated images. Our approach introduces the higher order cliques, energy into the co segmentation optimization process successfully. A region based likelihood estimation procedure is first performed to provide the primary knowledge for our higher order energy function. A new co segmentation energy function using higher order clique is developed, which can capably co segmentation energy function using higher order clique is developed, which can efficiently co segment the foreground objects with huge manifestation variations from a group of images in complex scenes. Both the quantitative and qualitative experimental results on representative datasets reveal that the accuracy of our co segmentation results is much higher than the state-of-the-art co segmentation methods.

Index Terms: Energy optimization, higher order cliques, image co segmentation, and likelihood estimation.

1. INTRODUCTION

IMAGE co-segmentation is commonly referred as jointly partitioning multiple images into foreground and background components. The idea of co-segmentation is first introduced by Rother et al. [5] where they simultaneously segment common foreground objects from a pair of images. The co-segmentation problem has attracted much attention in the last decade, most of the co-segmentation approaches are motivated by traditional Markov Random Field (MRF) based energy functions, which are generally solved by the optimization techniques

such as linear programming [8], dual decomposition [18] and network flow model [10]. The main reason may be that the graph-cuts and MRF methods [4], [33] work well for image segmentation and are also widely used to solve the combinatorial optimization problems in multimedia processing. Similar rationale is also adopted by some co-saliency methods [9], [42], [44].

The existing image co-segmentation methods can be roughly classified into two main categories, including unsupervised co segmentation techniques and interactive co-segmentation approaches. The common idea of the unsupervised techniques [5], [11], [16], [22], [27], [29], formulates image co segmentation as an energy minimization and binary labeling problem. These approaches usually define the energy function using standard MRF terms and histogram matching term. The former encourages the consistent segmentations in every single image while the later penalizes the differences between the foreground histograms of multiple images.

Inspired by interactive single-image segmentation methods [7], [15], [26], several interactive co-segmentation approaches [17], [19], [21], [28] using user scribbles have been proposed in recent years. The user usually indicates scribbles of foreground or background as additional constraint information to improve the co-segmentation performance. These interactive co segmentation approaches can handle a group of related images and improve the co-segmentation results by user scribbles. Batra et al. [19], [21] proposed an interactive image co-segmentation approach to segment foreground objects with user interactions. They learned

foreground/background appearance models using user scribbles. Recently, Collins et al. [28] formulated the interactive image co-segmentation problem as the random walk model and added the consistency constraint between the extracted objects from a set of input images. Their method utilized the normalized graph Laplacian matrix and solved the random walk optimization scheme by exploiting its quasi-convexity of foreground objects.

Higher Order Cliques

A class of higher order clique potentials and show that the expansion and swap moves for any energy function composed of these potentials can be found by minimizing a sub modular function. We also show that for a subset of these potentials, the optimal move can be found by solving a st-mincut problem. We refer to this subset as the Pn Potts model.

Image Co-Segmentation

Co-segmentation is the problem of simultaneously dividing q images into regions (segments) corresponding to k different classes. When $q = 1$ and $k = 2$, this reduces to the classical segmentation problem where an image is divided into foreground and background regions. Despite over 40 years of research, it is probably fair to say that there is still no reliable purely bottom-up single-image segmentation algorithm [9, 17, 22]. The situation is different when a priori information is available, for example in a supervised or interactive setting where labeled samples are available for the foreground and background (or even additional, $k > 2$) classes (see, e.g., [5, 6, 12]). The idea of co-segmentation is that the availability of multiple images that contain instances of the same “objects” classes makes up for the absence of detailed supervisory information.

Pn Potts Model

We now introduce the Pn Potts model family of higher order clique potentials. This family is a strict generalization of the Generalized Potts model [4] and can be used for modeling many problems in Computer Vision. We define the Pn Potts model potential for cliques of size n as

$$\psi_c(x_c) = \begin{cases} \gamma_k & \text{if } x_i = l_k, \forall i \in c \\ \gamma_{max} & \text{otherwise} \end{cases}$$

Where, $\gamma_{max} > \gamma_k, \forall k \in L$. For a pair wise clique this reduces to the P2 Potts model potential defined as $\psi_{ij}(a, b) = \gamma_k$ if $a = b = l_k$ and γ_{max} otherwise. If we use $\gamma_k = 0$, for all l_k , this function becomes an example of a metric potential function.

Most energy minimization based methods for solving Computer Vision problems assume that the energy can be represented in terms of unary and pair wise clique potentials. This assumption severely restricts the representational power of these models making them unable to capture the rich statistics of natural scenes. Higher order clique potentials have the capability to model complex interactions of random variables and thus could overcome this problem. Researchers have long recognized this fact and have used higher order models to improve the expressive power of MRFs and CRFs [15, 19, 20]. The initial work in this regard has been quite promising and higher order cliques have been shown to improve results. However their use has been quite limited due to the lack of efficient algorithms for minimizing the resulting energy functions.

2. OUR APPROACH

A. Overview

Our co-segmentation procedure includes two main steps. The first step is a fast but effective likelihood estimation process, which calculates the probabilities of pixels belonging to fore-ground/background over entire dataset according to user scribbles. The estimated likelihood offers a rough estimation for foreground /background and is fed into next step as prior knowledge. This process is described in Section II-B. In the second stage, a higher-order energy based co-segmentation function is proposed to obtain final accurate co-segmentation results on a group of images, which is based on higher order cliques. Our higher-order cliques are constructed from a set of foreground and background regions by user scribbles, where all the regions in each image are matched to produce better co-segmentation performance. Additionally, our approach considers the quality of

segmentation in higher-order energy to obtain more accurate estimations of foreground/background.

B. Likelihood Estimation

Given a group of images $\{I^1, \dots, I^n\}$ and the user scribbles that indicate foreground or background objects, we first compute pixel likelihood x_k^i for foreground/background in image I^i . The likelihood of pixel x_k^i is denoted by $\pi_{k,l}^i$ where l is a label indicating foreground (1) or background (0) and k is the index value of x_k^i . We compute the likelihoods of regions instead of pixels for computational efficiency. Each input image I^i of the group is divided into regions $r_s^i \in R^i$ using the over-segmentation methods such as mean shift [1] or efficient graph [6] method. For each region r_s^i , the region likelihoods of foreground and background are defined as $z_{s,l}^i$, which is further formulated in a quadratic energy function as follows:

$$F_l^i = F_1 + F_2$$

$$= \lambda^i \sum_{s=1}^{N(R^i)} (z_{s,l}^i - \epsilon_{s,l}^i)^2$$

$$+ \sum_{s,s'=1}^{N(R^i)} \omega_{s,s'}^i (z_{s,l}^i - z_{s',l}^i)^2 \dots \dots \dots 1$$

Where the first term F_1 defines a unary constraint that each region tends to have the initial likelihood $\epsilon_{s,l}^i$ estimated through the appearance similarity to foreground/background. The second term F_2 gives the interactive constraint that all regions of the whole image should have same likelihood when their representative colors are similar.

The parameter λ is a positive coefficient for balancing the relative influence between F_1 and F_2 . $\omega_{s,s'}^i = \exp(-\|c_s^i - c_{s'}^i\|)$ is a weighting function that gives a similarity measure for regions r_s^i and $r_{s'}^i$ in color space, and \bar{c}_s^i is the mean color of region r_s^i . $N(R^i)$ is the number of regions of R^i and the

parameter $z_{s,l}^i$ indicates the likelihood of region r_s^i . $\epsilon_{s,l}^i$ defines the initial likelihood for region r_s^i .

Given the user scribbles, we can get the background region set $U_j \in U^{(0)}$ and foreground region set $U_{s'} \in U^{(1)}$. We use the shortest Euclidean distance between region r_s^i and the background/foreground region set (U_0/U_1) in color space to compute the initial likelihood $\epsilon_{s,l}^i$ for region r_s^i . The initial likelihood $\epsilon_{s,l}^i$ is formulated as

$$\epsilon_{s,l}^i = \begin{cases} \frac{\min_{u_j \in U_0} (\|c_s^i - \bar{c}_j\|)}{\min_{u_j \in U_0} (\|c_s^i - \bar{c}_j\|) + \min_{u_j \in U_1} (\|c_s^i - \bar{c}_j\|)} & \text{if } l = 1 \\ \frac{\min_{u_{j'} \in U_1} (\|c_s^i - \bar{c}_{j'}\|)}{\min_{u_j \in U_0} (\|c_s^i - \bar{c}_j\|) + \min_{u_{j'} \in U_1} (\|c_s^i - \bar{c}_{j'}\|)} & \text{if } l = 0 \end{cases} \dots (2)$$

Where \bar{c}_j ($\bar{c}_{j'}$) is the mean color of background region u_j (foreground region $u_{j'}$). Based on the region likelihoods $z_l^i = [z_{s,l}^i] N(R^i) \times 1$ and their initial region likelihoods $\epsilon_l^i = [\epsilon_{s,l}^i] N(R^i) \times 1$, the quadratic energy function F_1 is formulated as the following matrix forms:

$$F_l^i = (\bar{z}_l^i - \bar{\epsilon}_l^i)^T \Lambda^i (\bar{z}_l^i - \bar{\epsilon}_l^i) + \bar{z}_l^{i,T} (D^i - W^i) \bar{z}_l^i \quad (3)$$

Where $W^i = [w_{s,s'}^i] N(R^i) \times N(R^i)$ and $D^i = \text{diag}([d_1^i, \dots, d_N^i(R^i)])$. The diagonal elements of the metric D^i are the degrees of the weight matrix w^i : $d_s^i = \sum_{s'=1}^{N(R^i)} \omega_{s,s'}^i$. The diagonal elements of the metric Λ^i are $\text{diag}([\lambda^1, \dots, \lambda^i]) N(R^i) \times N(R^i)$.

(3) is then solved by the following convex optimization:

$$\frac{\partial F_l^i}{\partial \bar{z}_l^i} = \Lambda^i (\bar{z}_l^i - \bar{\epsilon}_l^i) + (D^i - W^i) \bar{z}_l^i = 0 \quad (4)$$

After solving (4), we finally obtain the region likelihoods \bar{z}_l^i as follows:

$$\bar{z}_l^i = \frac{\Lambda^i \bar{\epsilon}_l^i}{\Lambda^i + D^i - W^i} \quad (5)$$

Considering the definition of $\varepsilon_{s,l}^i$ in (2), we have $\varepsilon_{s,0}^i + \varepsilon_{s,1}^i = 1$. According to $\varepsilon_{s,0}^i + \varepsilon_{s,1}^i = 1$ and (5), we have

$$z_{s,0}^i + z_{s,1}^i = 1 \quad (6)$$

We only need to calculate either \bar{z}_0^i or \bar{z}_1^i using (5). (5) is easily computed by least-square and the optimization only takes 0.02 s for 500 over-segmentation regions per image in our tests. After the region likelihood \bar{z}_l^i is obtained, the pixel likelihood $\pi_{k,l}^i$ is set to the same value as the likelihood of the region that this pixel belongs to

$$\pi_{k,l}^i = z_{s^k,l}^i$$

Where s^k indicates the region $r_{s^k}^i$ that pixel x_k^i belongs to.

3. PROPOSED METHOD

Higher-Order Energy Co-Segmentation

Via our likelihood estimation, we have a fast and rough estimate for foreground/background in each image. For generating more accurate co-segmentation results, we further propose a higher-order energy based co-segmentation function.

In order to simultaneously segment a group of input images $\{I^1, \dots, I^n\}$ with the labeled images T, we first build a global term $E_{global}(I^1, \dots, I^n, T)$ to match all the images with the labeled images T. The proposed energy of our co-segmentation algorithm is expressed as follows:

$$\mathcal{F} = \sum_{i=1}^n (\epsilon_1^i E_{unary}^i + \epsilon_2^i E_{pairwise}^i) + E_{global}(I^1, \dots, I^n, T) \quad (7)$$

Where E_{unary}^i and $E_{pairwise}^i$ denote unary term and pairwise term respectively and the global term E_{global} is proposed to match all the input images $\{I^1, \dots, I^n\}$ with labeled images T. The scalars weight various terms.

The unary term E_{unary}^i and the pairwise term $E_{pairwise}^i$ for image I^i are defined as follows:

$$E_{unary}^i = \sum_k -\log(\pi_{k,1}^i) \cdot \phi(x_k^i) - \log(\pi_{k,0}^i) \cdot (1 - \phi(x_k^i))$$

$$E_{pairwise}^i = \sum_{k,k' \in \mathfrak{N}} \|c_k^i - c_{k'}^i\| \cdot |\phi(x_k^i) - \phi(x_{k'}^i)| \quad \dots \dots \dots (8)$$

Where c_k^i denotes the color value of pixel x_k^i and $\pi_{k,1}^i$ is obtained in our likelihood estimation step. The set \mathfrak{N} contains all the four-neighbors within one image. $\phi(x_k^i)$ is a binary function indicating the assignment of pixel x_k^i to the background (0) or foreground (1).

The unary term E_{unary}^i is based on the likelihood estimation results and penalizes assignments of pixels with lower likelihood to foreground. The pairwise term $E_{pairwise}^i$ imposes intra-image label smoothness by constraining the segmentation labels to be consistent, which tends to assign the same label to neighboring pixels that have similar color.

The co-segmentation model in (7) is intuitive. Next we discuss how to design the global energy item in the following paragraphs. Previous co-segmentation approaches [5], [10] performed co-segmentation on image pairs and made simple assumption that two input images shared a same/similar foreground object. In contrast, we try to extract common foreground objects that have large variations in color, texture and shape from a group of images with complex background. Rather than building a simple foreground or background appearance model, we collect a region set \mathfrak{S} of foreground/background according to user interaction. The region set of foreground/background.

Consists of the labeled regions U^l .

$$\mathfrak{S} = \{U^0, U^1\}$$

Where U^0/U^1 means the background/foreground regions respectively. The construction process of \mathfrak{S} is accomplished by the previous likelihood estimation step, and all the regions with user scribbles are added into this region set \mathfrak{S} . Fig. 2 gives the process of

obtaining the region set \mathfrak{S} from user seeds. In order to build the matching relationships between input images $\{I^1, \dots, I^n\}$ and labeled foreground/background images T , our solution is to make the matching process between the over-segmentation regions R^i of image I^i and the labeled regions from region set \mathfrak{S} .

The construction process of \mathfrak{S} is accomplished by the previous likelihood estimation step, and all the regions with user scribbles are added into this region set \mathfrak{S} . Fig. 2 gives the process of obtaining the region set \mathfrak{S} from user seeds. In order to build the matching relationships between input images $\{I^1, \dots, I^n\}$ and labeled foreground/background images T , our solution is to make the matching process between the over-segmentation regions R^i of image I^i and the labeled regions from region set \mathfrak{S} . Then we define the following higher-order energy item:

$$E_{global}(I^1, \dots, I^n, T) = \sum_{i=1}^n E_{High}(R^i, \mathfrak{S})$$

By associating with (8) and (9), our co-segmentation energy function F in (7) is then rewritten as

$$F = \sum_{i=1}^n \left\{ \sum_k \left(\exp^{-\pi^i_{k,1}} \phi(x_k^i) + \exp^{-\pi^i_{k,0}} (1 - \phi(x_k^i)) \right) + \sum_{k, k' \in N} \|c_k^i - c_{k'}^i\| \cdot |\phi(x_k^i) - \phi(x_{k'}^i)| + E_{High}(R^i, \mathfrak{S}) \right\} \quad (10)$$

The minimization of unary term and pairwise term in F (11) can be efficiently solved by the graph cut algorithm. Then we focus on how to design the higher-order term $E_{High}(R^i, \mathfrak{S})$ of I^i . We will introduce the higher-order cliques into matching process. The higher-order cliques are composed of three regions: the foreground region, the background region and the over-segmentation region. The co-segmentation process using higher-order energy is shown in Fig. 3. Both the foreground region and the

background region are selected to construct our region set \mathfrak{S} . Then we build a higher-order energy function $E_{High}(R^i, \mathfrak{S})$ on higher-order cliques as follows:

$$v_s^i = \{r_s^i, u^1(r_s^i), u^0(r_s^i)\} \dots \dots \dots (11)$$

where $u^l(r_s^i) \in U_1$ denotes the most related foreground or background region to r_s^i in Euclidean distance measurement using their mean colors.

For each region r_s^i of image I^1 , our algorithm finds the most similar foreground and background region from \mathfrak{S} respectively to make up a higher-order clique. Then the matching energy function using our higher-order cliques is defined as follows:

$$E_{High}(R^i, \mathfrak{S}) = \sum_{s=1}^{N(R^i)} N(v_s^i) \cdot k_s^i \dots \dots \dots (12)$$

Where $N(v_s^i)$ indicates the number of pixels in clique v_s^i , which means a large clique will have a large value of weight. k_s^i defines the matching coefficient which considers both the clique likelihood for foreground/background and the segmentation quality. We define the matching coefficient k_s^i as follows:

$$k_s^i = \min \left\{ \min \left(z^1(v_s^i) \cdot \vartheta^l(v_s^i) + z^{\bar{1}}(v_s^i) \right), 1 \right\} \dots \dots \dots (13)$$

Where $z^1(v_s^i)$ is the clique likelihood estimated from v_s^i , which is compute via

$$z^1(v_s^i) = \frac{N(r_s^i)^{z_{s,l}^i} + N(u^1(r_s^i))^l + N(u^0(r_s^i))^{(1-l)}}{N(r_s^i) + N(u^1(r_s^i)) + N(u^0(r_s^i))} \dots \dots \dots (14)$$

The parameter $\vartheta^l(v_s^i)$ in (13) is used to estimate the segmentation quality, which is based on region consistency assumption. The region consistency assumption encourages all pixels belonging to a region to take the same label. We define $\vartheta^l(v_s^i)$ as follows:

$$\vartheta^l(v_s^i) = \frac{N(r_s^i) - N_l(r_s^i)}{\rho^N(r_s^i)}, 0 < \rho < 1 \dots \dots \dots (15)$$

Where $N_l(r_s^i)$ is the number of pixels assigned to foreground/background in region r_s^i . We commonly set $\rho = 0.1$ in our experiments. That means, if more than 90% of the pixels in region r_s^i are classified into foreground, the value of $\vartheta^l(v_s^i)$ is less than 1. Similarly, if 50% of the pixels in region r_s^i are classified into foreground, the value of $\vartheta^l(v_s^i)$ is set to 5.

According to definition in (15), the more pixels of a region have the same label, the better segmentation quality on this region and the smaller value of $\vartheta^l(v_s^i)$ will be. Our higher-order energy function in (13) is a linear truncated function, which means that the higher-order energy function allows some pixels of a region to take different labels.

In clique v_s^i , we only need to consider the segmentation quality on region r_s^i because pixels in region $u^1(r_s^i)$ or $u^0(r_s^i)$ have been classified into foreground or background. Therefore, the more pixels in region r_s^i are divided into a same label, the higher segmentation quality is obtained and the lower the value of $\vartheta^l(v_s^i)$. From (14) and (15), we can find that the number of pixels in foreground/background $N(U^l(r_s^i))$ can influence the clique likelihood and the value of matching co-efficient k_s^i . Then we set $(U^l(r_s^i)) = 0.5 N(r_s^i) \mathcal{E}_{s,l}^i$. If region r_s^i is closer to foreground, $\mathcal{E}_{s,1}^i$ is larger and $N(U^l(r_s^i))$ will make a greater influence on the matching co-efficient k_s^i .

Higher-order energy function in (13) utilizes clique likelihood $z^l(v_s^i)$ for foreground and background. The region consistency in our higher-order clique is also taken into account as an evaluation for segmentation quantity $\vartheta^l(v_s^i)$. In other words, our higher-order energy function considers the similarity between higher-order clique and foreground/background, which encourages all the pixels of a region to take the same label. Next we will introduce our optimization method for higher-order energy in (13). Because the value of $N_l(r_s^i)$ is constant, the problem of minimizing our higher-order energy function can be transformed into a problem of minimizing the matching co-efficient k_s^i , which is defined in the following two important theorems.

Theorem 1: The matching coefficient k_s^i in (13) can be rewritten as

$$k_s^i = \min \left\{ \frac{\sum_{x_s^i \in r_s^i} \phi(x_s^i)}{Q} (1-t) + t, \frac{N(r_s^i) - \sum_{x_s^i \in r_s^i} \phi(x_s^i)}{Q} t + (1-t) \right\}$$

Where $t = z^1(\vartheta_s^i)$, $Q = \rho N(r_s^i)$ and pixel x_s^i belongs to region r_s^i . $\phi(\cdot)$ is the binary function indicating the assignment of pixel to background (0) or foreground (1) in (8).

Theorem 2: The matching coefficient k_s^i in (16) can be transformed into a second-order function by introducing the auxiliary binary variables σ_0 and σ_1 .

$$k_s^i = \min \Psi(\sigma_0, \sigma_1, \phi(x_s^i)) = \min_{\sigma_0, \sigma_1} \left\{ \sigma_0 \frac{\sum_{x_s^i \in r_s^i} \phi(x_s^i)}{Q} (1-t) + (1-\sigma_0)(1-t) + \sigma_1 \frac{N(r_s^i) - \sum_{x_s^i \in r_s^i} \phi(x_s^i)}{Q} t + (1-\sigma_1)t \right\} \quad (17)$$

The proofs of Theorem 1 and Theorem 2 are given in detail in Appendix A and Appendix B. Through Theorem 1 and Theorem 2, the matching coefficients k_s^i in (13) can be rewritten as a second-order function. Therefore, our higher-order energy based co-segmentation function in (7) can be efficiently solved by the conventional graph cut algorithm.

4. SIMULATION RESULTS

In this section, we first discuss our experiments for evaluating the performance between our algorithm and previous well-known co-segmentation approaches. Then, we give qualitative and quantitative results obtained by the proposed method with and without the higher-order energy. The experimental evaluations are designed to assess the running time statistics of these algorithms. Then, we give qualitative and quantitative results obtained by

the proposed method with and without the higher-order energy. The experimental evaluations are designed to assess the running time statistics of these algorithms. Three parameters λ , 1 and 2 are used in our two energy functions (1) and (7). We empirically set $\lambda = 10$, 1 = 1 and 2 = 30 for all the test image sets in our experiments.

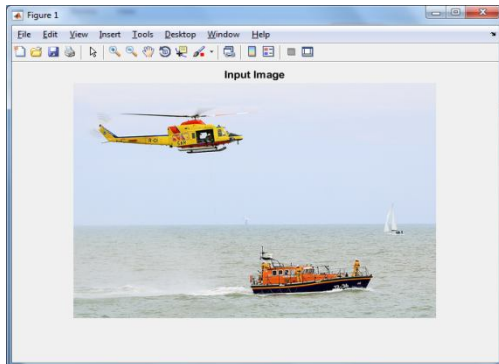


Fig.1. The input image

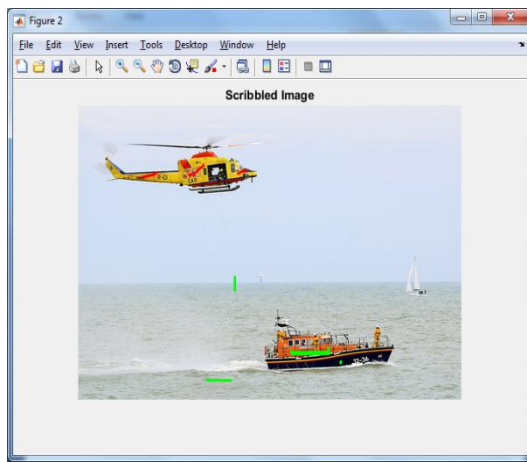


Fig.2. scribbled image

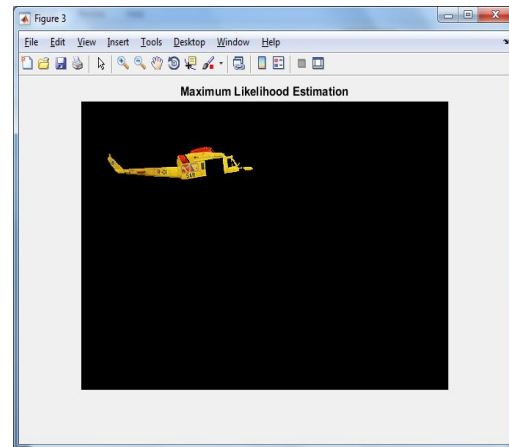


Fig.3. likelihood estimation

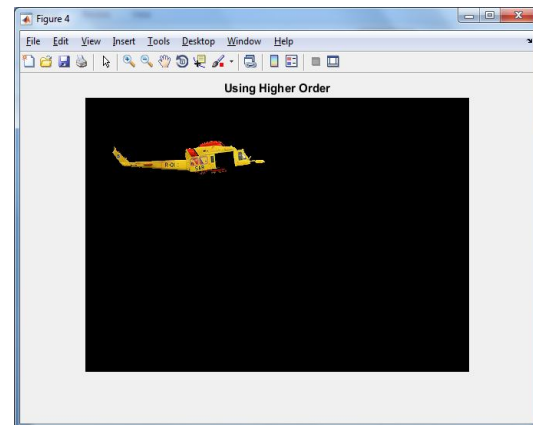


Fig.4. our purposed method using Higher order co-segmentation

Our method is first compared with the state-of-the-art interactive co-segmentation methods: intelligent scribble guided co-segmentation (ICOSEG) [21], and RWCS [28] on previous benchmark datasets. To achieve a relatively fair comparison, both the proposed method and other interactive co-segmentation methods [21], [28] use the same scribbles in all experiments.

5. CONCLUSION

We have presented a novel interactive co-segmentation approach using the likelihood estimation and high-order energy optimization to extract the complicated foreground objects from a group of related images. A likelihood estimation method is developed to compute the prior knowledge

for our higher-order co-segmentation energy function. Our higher-order cliques are built on a set of foreground and background regions obtained by likelihood estimation. Then our co-segmentation process from a group of images is performed at the region level through our higher-order cliques energy optimization. The energy function of our higher-order cliques can be further transformed into a second-order Boolean function and thus the traditional graph cuts method can be used to solve them exactly. The experimental results demonstrated both qualitatively and quantitatively that our method has achieved more accurate co-segmentation results than previous unsupervised and interactive co-segmentation methods even though the foreground and background have many overlap regions in color distributions or in very complex scenes.

REFERENCES

- [1] D. Comaniciu and P. Meer, "Mean shift: A robust approach toward feature space analysis," *IEEE Trans. Pattern Anal. Mach. Intell.*, vol. 24, no. 5, pp. 603–619, May 2002.
- [2] Z. Lou and T. Gevers, "Extracting primary objects by video cosegmentation," *IEEE Trans. Multimedia*, vol. 16, no. 8, pp. 2110–2117, Dec. 2014.
- [3] C. Wang, Y. Guo, J. Zhu, L. Wang, and W. Wang, "Video object cosegmentation via subspace clustering and quadratic pseudo-boolean optimization in an MRF framework," *IEEE Trans. Multimedia*, vol. 16, no. 4, pp. 903–916, Jun. 2014.
- [4] V. Kolmogorov and R. Zabih, "What energy functions can be minimized via graph cuts?" *IEEE Trans. Pattern Anal. Mach. Intell.*, vol. 26, no. 2, pp. 147–159, Feb. 2004.
- [5] C. Rother, T. Minka, A. Blake, and V. Kolmogorov, "Cosegmentation of image pairs by histogram matching-incorporating a global constraint into MRFs," in *Proc. IEEE Conf. Comput. Vis. Pattern Recog.*, 2006, pp. 993–1000.
- [6] P. Felzenszwalb and D. Huttenlocher, "Efficient graph-based image segmentation," *Int. J. Comput. Vis.*, vol. 59, no. 2, pp. 167–181, 2004.
- [7] Y. Boykov and G. Funka-Lea, "Graph cuts and efficient n-d image segmentation," *Int. J. Comput. Vis.*, vol. 70, no. 2, pp. 109–131, 2006.
- [8] L. Mukherjee, V. Singh, and C. R. Dyer, "Half-integrality based algorithms for cosegmentation of images," in *Proc. IEEE Conf. Comput. Vis. Pattern Recog.*, Jun. 2009, pp. 2028–2035.
- [9] W. Wang, J. Shen, and L. Shao, "Consistent video saliency using local gradient flow optimization and global refinement," *IEEE Trans. Image Process.*, vol. 24, no. 11, pp. 4185–4196, Nov. 2015.
- [10] D. S. Hochbaum and V. Singh, "An efficient algorithm for cosegmentation," in *Proc. IEEE Int. Conf. Comput. Vis.*, Sep.-Oct. 2009, pp. 269–276.
- [11] H. Fu, D. Xu, S. Lin, and J. Liu, "Object-based RGBD image cosegmentation with Mutex constraint," in *Proc. IEEE Conf. Comput. Vis. Pattern Recog.*, Jun. 2015, pp. 4428–4436.
- [12] P. Kohli, L. Ladicky, and P. Torr, "Robust higher order potentials for enforcing label consistency," *Int. J. Comput. Vis.*, vol. 82, no. 3, pp. 302–324, 2009.
- [13] W. Wang, J. Shen, X. Li, and F. Porikli, "Robust video object cosegmentation," *IEEE Trans. Image Process.*, vol. 24, no. 10, pp. 3137–3148, Oct. 2015.
- [14] I. Hiroshi, "Higher-order clique reduction in binary graph cut," in *Proc. IEEE Conf. Comput. Vis. Pattern Recog.*, Jun. 2009, pp. 2993–3000.
- [15] V. Gulshan, C. Rother, A. Criminisi, A. Blake, and A. Zisserman, "Geodesic star convexity for interactive image segmentation," in *Proc. IEEE Conf. Comput. Vis. Pattern Recog.*, Jun. 2010, pp. 3129–3136.
- [16] A. Joulin, F. Bach, and J. Ponce, "Discriminative clustering for image cosegmentation," in *Proc. IEEE Conf. Comput. Vis. Pattern Recog.*, Jun. 2010, pp. 1943–1950.
- [17] X. Dong, J. Shen, L. Shao, and M. H. Yang, "Interactive co-segmentation using global and local energy optimization," *IEEE Trans. Image Process.*, vol. 24, no. 11, pp. 3966–3977, Nov. 2015.
- [18] S. Vicente, V. Kolmogorov, and C. Rother, "Cosegmentation revisited: Models and optimization," in *Proc. Eur. Conf. Comput. Vis.*, 2010, pp. 465–479.
- [19] D. Batra, A. Kowdle, D. Parikh, J. Luo, and T. Chen, "iCoseg: Interactive co-segmentation with intelligent scribble guidance," in *Proc. IEEE Conf. Comput. Vis. Pattern Recog.*, Jun. 2010, pp. 3169–3176.

- [20] T. H. Kim, K. M. Lee, and S.U. Lee, "Nonparametric higher-order learning for interactive segmentation," in Proc. IEEE Conf. Comput. Vis. Pattern Recog., Jun. 2010, pp. 3201–3208.
- [21] D. Batra, A. Kowdle, D. Parikh, J. Luo, and T. Chen, "Interactively cosegmenting topically related images with intelligent scribble guidance," Int. J. Comput. Vis., vol. 93, pp. 273–292, 2011.
- [22] G. Kim, E. P. Xing, L. Fei-Fei, and T. Kanade, "Distributed cosegmentation via submodular optimization on anisotropic diffusion," in Proc. IEEE Int. Conf. Comput. Vis., Nov. 2011, pp. 169–176.
- [23] L. Mukherjee, V. Singh, and J. Peng, "Scale invariant cosegmentation for image groups," in Proc. IEEE Conf. Comput. Vis. Pattern Recog., Jun. 2011, pp. 1881–1888.
- [24] K. Chang, T. Liu, and S. Lai, "From co-saliency to co-segmentation: An efficient and fully unsupervised energy minimization model," in Proc. IEEE Conf. Comput. Vis. Pattern Recog., Jun. 2011, pp. 2129–2136.
- [25] A. C. Gallagher, D. Batra, and D. Parikh, "Inference for order reduction in Markov random fields," in Proc. IEEE Conf. Comput. Vis. Pattern Recog., Jun. 2011, pp. 1857–1864.
- [26] B. Cheng, G. Liu, J. Wang, Z. Huang, and S. Yan, "Multi-task low-rank affinity pursuit for image segmentation," in Proc. IEEE Int. Conf. Comput. Vis., Nov. 2011, pp. 2439–2446.
- [27] A. Joulin, F. Bach, and J. Ponce, "Multi-class cosegmentation," in Proc. IEEE Conf. Comput. Vis. Pattern Recog., Jun. 2012, pp. 542–549.
- [28] M. D. Collins, J. Xu, L. Grady, and V. Singh, "Random walks based multi-image segmentation: Quasiconvexity results and GPU-based solutions," in Proc. IEEE Conf. Comput. Vis. Pattern Recog., Jun. 2012, pp. 1656–1663.
- [29] Y. Chai, V. Lempitsky, and A. Zisserman, "BiCoS: A bi-level cosegmentation method for image classification," in Proc. IEEE Int. Conf. Comput. Vis., Nov. 2011, pp. 2579–2586.
- [30] J. Shotton, J. Winn, C. Rother, and A. Criminisi, "TextonBoost: Joint appearance, shape and context modeling for multi-class object recognition and segmentation," in Proc. Eur. Conf. Comput. Vis., 2006, pp. 1–15.

- [31] H. Ishikawa, "Higher-order vlique reduction in binary graph cut," in Proc. IEEE Conf. Comput. Vis. Pattern Recog., Jun. 2009, pp. 2993–3000.
- [32] H. Ishikawa, "Transformation of general binary MRF minimization to the first order case," IEEE Trans. Pattern Anal. Mach. Intell., vol. 33, no. 6, pp. 1234–1249, Jun. 2011.
- [33] C. Couprie, L. Grady, L. Najman, and H. Talbot, "Power watersheds: A new image segmentation framework extending graph cuts, random walker and optimal spanning forest," in Proc. IEEE Int. Conf. Comput. Vis., Sep.- Oct. 2009, pp. 731–738.
- [34] K. Park and S. Gould, "On learning higher-order consistency potentials for multi-class pixel labeling," in Proc. Eur. Conf. Comput. Vis., 2012, pp. 202–215.

FACULTY DETAILS:



NAME: Ummadi Sathish Kumar

Mr. Ummadi Sathish Kumar educational qualification is M.Tech (Ph.d). Presently his working as a Assistant Professor in Acharya nagarjuna university college of engineering & technology. So far he is working as teaching experience of 10 years in computer science and engineering. His special fields of interest in Data Mining, Image processing, Soft Computing.

STUDENT DETAILS:



NAME: KULLI JOSHIBABU

Mr. Kulli Joshibabu educational qualification is B.Tech in Bapatla Engineering college, Bapatla. His special fields of Interest in soft computing, machine learning and image processing.